EVN Doc. n. 75

High Dynamic Range Imaging with the EVN

M. Massi and S. Aaron
Joint Institute for VLBI in Europe. Postbus 2, 7990 AA, Dwingeloo, The Netherlands
Max-Planck-Institut für Radioastronomie, Auf dem Hügel 69, D-53121 Bonn, Germany

1. Introduction

It is fairly well known that images obtained with EVN arrays do not achieve the dynamic range that one would expect from standard calculations of the thermal noise. In order to understand the limiting factors of the EVN, we have been carefully analyzing data obtained on the bright, compact radio source DA 193. The source was observed on 30 May 1995 for twelve hours in Mark III mode A with the Effelsberg, Jodrell Bank, Medicina, Noto, Onsala, Crimea, Westerbork, Shanghai, and Urumqi stations. No correlated data were obtained on baselines to the latter two stations. Three stations recorded dual polarization, the remaining recorded LCP. Cross polarized correlations were obtained where possible. Analysis of these data have demonstrated two effects which provide the predominant causes of baseline errors in EVN data: instrumental polarization (Massi et al. 1996; Massi et al. 1997) and the variable amplitude attenuation due to the discrete delay tracking (Leppänen et al. 1997). In this memo we report the current status of this project, with the appropriate corrections for these effects applied.

2. Noise comparison

The theoretical noise in a naturally weighted image is given by (Walker 1989)

$$\Delta I = \frac{\eta}{\sqrt{\sum \frac{1}{\Delta A^2}}} \tag{1}$$

where the only loss factor η that will be taken into account is that due to the one-bit sampling. The expected baseline sensitivity

$$\Delta A_{ij} = \frac{1}{\sqrt{2\Delta\nu\tau}}\sqrt{\frac{T_{sys_i}T_{sys_j}}{G_iG_j}} \tag{2}$$

has been computed for our data using the average value of the system temperature for the 48 scans and the 14 recorded IF's at each station. These averaged values for each station and the relative gain are listed in Table 1. By assuming that all the 7 antennas were simultaneously observing in each of the 48 scans, each lasting 13 minutes, the predicted noise in the image is, from Equation 1,

$$\Delta I_{\rm Walker} = 0.064 \text{ mJy beam}^{-1} \ . \tag{3}$$

In order to precisely determine the expected noise in our image, we have simulated our observation by using the Caltech program FAKE and generated artificial data at the observed uv points with added thermal noise. The estimated noise in the image calculated by the DIFMAP program is

$$\Delta I_{\rm sim} = 0.086 \text{ mJy beam}^{-1} \tag{4}$$

for natural weighting and 0.23 mJy beam^{-1} for uniform.

Initially, we processed the DA 193 data normally, i.e. we used a version of AIPS that did not compensate the variable fractional bit shift amplitude loss and we did not calibrate and correct for the instrumental polarization. Making the Stokes LL image from these data, we find an RMS noise of 1.2 mJy beam^{-1} for both natural and uniform weighting. As the noise is insensitive to the weighting scheme used in the imaging, we may immediately conclude that the imaging is significantly limited by baseline errors. We quantify the degradation in the image by taking the ratio of the measured and expected noise in the image: $\delta = 1.2/0.23 = 5.2$ for uniform weighting and $\delta = 14$ for natural.

After correction of the data for the effects of instrumental polarization (Massi et al, 1997a; Massi et al, 1997b) and for the FBS amplitude loss (Leppänen et al. 1997), the noise in the naturally weighted image (Figure 1) reduces to 0.16 mJy beam^{-1} and in the uniformly weighted image to 0.36 mJy beam^{-1}. Versions of the AIPS tasks MK3IN and SPLIT which apply these corrections are available with release 15OCT96 and later. Thus, the degradation factor in the image has reduced to $\delta = 1.9$ for natural weighting and $\delta = 1.6$ for uniform. *We conclude therefore that, at present, the degradation factor is reduced to a factor* ≤ 1.9.

Briggs et al (1994) and Cornwell et al (1995) have shown as the CLEAN algorithm itself limits the dynamic range. The authors do not explicitly quantify the degradations. However when we compare their maps produced with alternative methods came out a degradation factor of 1.4-1.6, reasonably compatible with our remaining factor. Is that true? Is our final map limited by the particular data processing (CLEAN) or are residual baseline errors the cause of the degradation? The proper answer can be found only by examining the $u-v$ data itself, through the closure phases.

3. Closure phase: Gaussian probability distribution vs histogram

In the hypothesis of no residual baseline errors, the closure phase contains information on the source structure plus noise contributions. If the observed source is strong and unresolved, the closure phase becomes equal to zero within the noise; its probability distribution is a Gaussian distribution centered at zero and with a standard deviation:

$$\Delta\theta_{ikm} = \sqrt{\left(\frac{1}{\mathrm{SNR}_{ik}}\right)^2 + \left(\frac{1}{\mathrm{SNR}_{km}}\right)^2 + \left(\frac{1}{\mathrm{SNR}_{im}}\right)^2} \tag{5}$$

In this section by overlaying the histograms of the observed closure phases with gaussians having the standard deviation predicted by Equation 5, we will immediately determine the extent of the remaining baseline errors in the data.

The SNR $= \frac{A}{\Delta A}$ can be again computed by using Equation 2 together with the observed total flux. However there is also an experimental estimation of the quantity SNR and is that delivered by the correlator fringe fitting program FRNGE. By dealing with samples of amplitude and phase (derived at the proper delay/rate which maximizes the correlation function), each with an integration time of 4 seconds, FRNGE computes the standard deviation on the whole scan length. In Figure 2 we show, as an example the plots of the quantity SNR derived by FRNGE as a function of time. For each scan we have one value of the SNR quantity (just the inverse of the standard deviation, computed over a scan, of the phase). There are therefore 48 measurements of SNR. For each baseline we have computed the average of that values and the relative dispersion given in column 1 and 2 of Table 2. In column 3 we give the "expected" value computed with Equation 2 and the integrated flux density of DA 193. Other than the baselines with Crimea, the agreement between expected and measured SNR is a such that we may conclude that *within the scan length of 13 minutes, no significant variation of baseline error is present.*

In Figures 3a and 3b, we show the histograms of closure phase overlayed with the theoretic gaussian. The proved agreement between observed and expected values for the SNR allows us to assume as highly reliable the standard deviation $\Delta\theta$ of the gaussians computed by Equation 5.

We see that residuals are still present. The accurate analysis of the plots will be given in the next memo. However we note here that the average closure phase is 0.27° and the average "standard deviation" of the gaussians (that is the predicted noise) is 0.14°. Can be a such small offset be responsible of the remaining degradation of the dynamic range determined in the previous section? Perley (1986) has shown as the dynamic range is inversely related to phase errors. The dynamic range degradation respect to an image only noise-limited can be therefore estimated from the ratio of the offset of 0.27° with respect to the noise : $0.27/0.14 = 1.9$. And even if one deletes baselines with Crimea, one finds a ratio of $0.18/0.10 = 1.8$.

The fact that the source is mildly resolved (model fitting to the $u-v$ data gives a gaussian of 0.96×0.55 mas) at our resolution has been considered by resimulating the data with this gaussian model rather than the point source used above. The closure phase distribution for these data still show less spread than in the observations; the closure phase of simulated data is confined within the gaussian distribution assumed above. We conclude that the deviations shown in Figures 3a and 3b are due to residual baseline errors in the data and not due to source structure.

4. Conclusions

1) Due to the high instrumental polarization of some of the European telescopes and to the non-correction for the FBS amplitude loss, the images produced up to now with EVN data had a dynamic range degradation up to a factor 14.

2) The dynamic range degradation drops to a factor 2 once the two aforementioned corrections are applied. The dynamic range in the final map is 39187 while the theoretical one for a noise limited image is 72906.

3) CLEAN limitations and residual errors can together give rise to the final degradation. However, the analysis reported here suggests that the residual errors are primarily responsible.

5. Future Work

These data are being recorrelated on the VLBA correlator in Socorro. This will allow a detailed comparison of the Mark III and VLBA systems, which may reveal further baseline errors arising in the Bonn correlator; baseline errors are known to be very small for the VLBA correlator.

Acknowledgements Maria Massi acknowledges support for her research by the European Union under contract FMGECT950012. Scott Aaron acknowledges support for his research by the European Union under contract CHGECT920011.

Table 1. Gain and system temperature measurements for the EVN stations used in this observation.

	Antenna Code						
	B	J	L	N	S	W	C
T_{sys}	88	55	54	49	96	195	154
Gain	1.386	0.111	0.160	0.141	0.045	1.000	0.067
SEFD	63	496	339	348	2147	195	2299

Table 2. Expected and measured baseline SNR.

Baseline	Measured SNR (scatter)	Expected SNR
JL	1922 (334.)	1918
JN	1723 (214.)	1891
JS	736 (186.)	762
JW	2395 (103.)	2527
BJ	4309 (419.)	4428
BL	5644 (338.)	5362
BN	5356 (600.)	5287
BS	2176 (392.)	2129
BW	7043 (474.)	7065
LN	2304 (296.)	2290
LS	941 (341.)	922
LW	2970 (281.)	3059
NS	785 (317.)	909
NW	2923 (180.)	3017
SW	1165 (334.)	1215
NC	659 (172.)	879
SC	282 (67.)	354
WC	856 (39.)	1174
BC	1572 (103.)	2058
JC	523 (100.)	736
LC	726 (142.)	891

REFERENCES

Briggs, D. S., Davis, R. J., Conway, J. E., Walker, R. C. 1994, July 25, VLBA memo 697

Cornwell, T. J., Kemball, A. J., & Benson , J. M. 1995, July 5, VLBA memo n.11

Leppänen, K., Massi, M., Rioja, M., Sanghera, H. 1997, to appear in the *Proceedings of the 3rd EVN/JIVE Symposium*, ed. F. Colomer and M. Garrett.

Massi, M., Comoretto, G., Rioja, M., & Tofani, G. 1996, *Astron. & Astrophys. Suppl.* **116**:167.

Massi, M., Rioja, M., Gabuzda, D., Leppänen, K., Sanghera, H., Ruf, K., & Moscadelli, L. 1997, *Astron. & Astrophy.* **318**:L32

Perley, R. A.: 1986, Synthesis Imaging, proc. NRAO. eds R. A. Perley, F.R. Schwab and A. H. Bridle, p.290

Walker , R. C. 1989. VLBI Techniques and Applications. ed. Delli and Spencer. Kluwer Academic Pub. p. 179

This preprint was prepared with the AAS LaTeX macros v4.0.

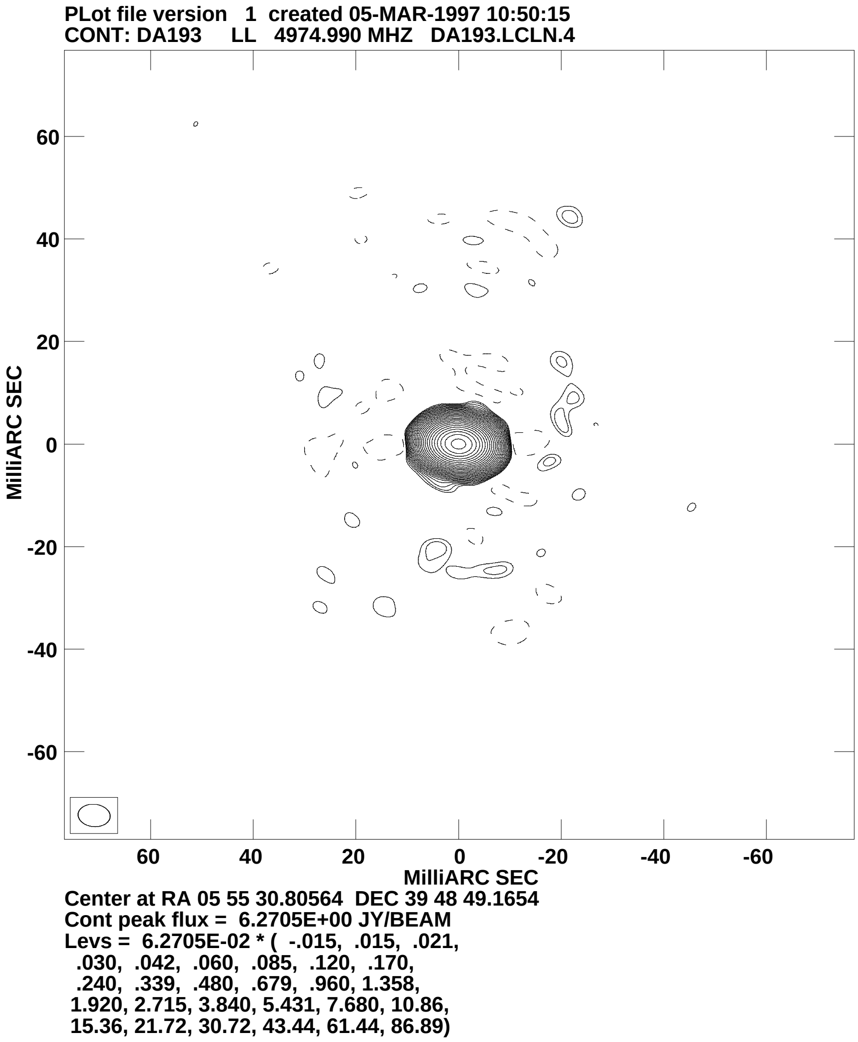

Fig. 1.— Naturally weighted image of DA 193, Stokes parameter LL. The contours are of total intensity at -0.015, 0.015, 0.021, 0.03, 0.042, ..., and 86.89% of the peak flux of 6.27 Jy beam^{-1}. The restoring beam is 6.26×4.37 mas oriented at 84.8°.

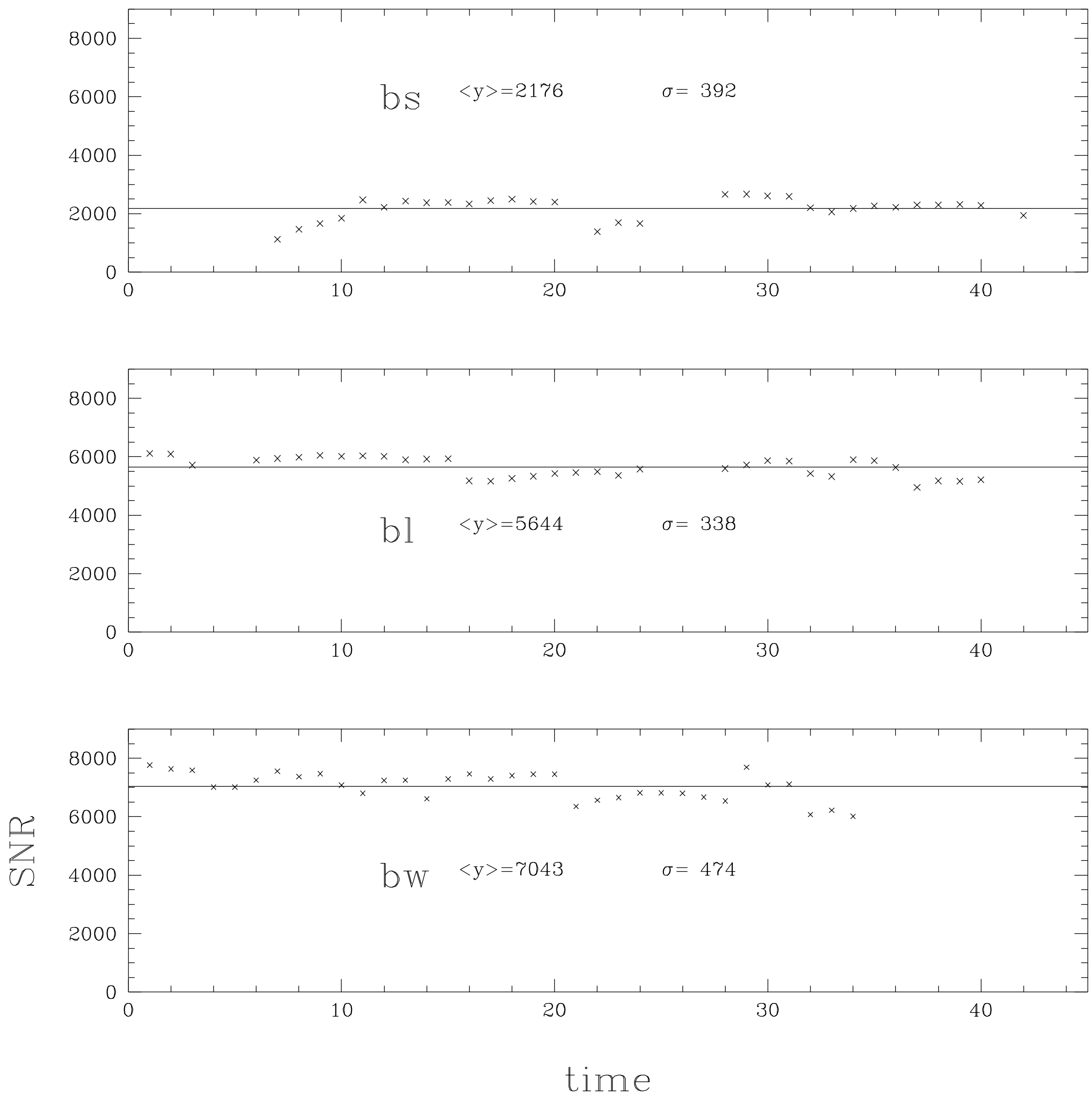

Fig. 2.— SNR delivered by the program FRNGE vs time

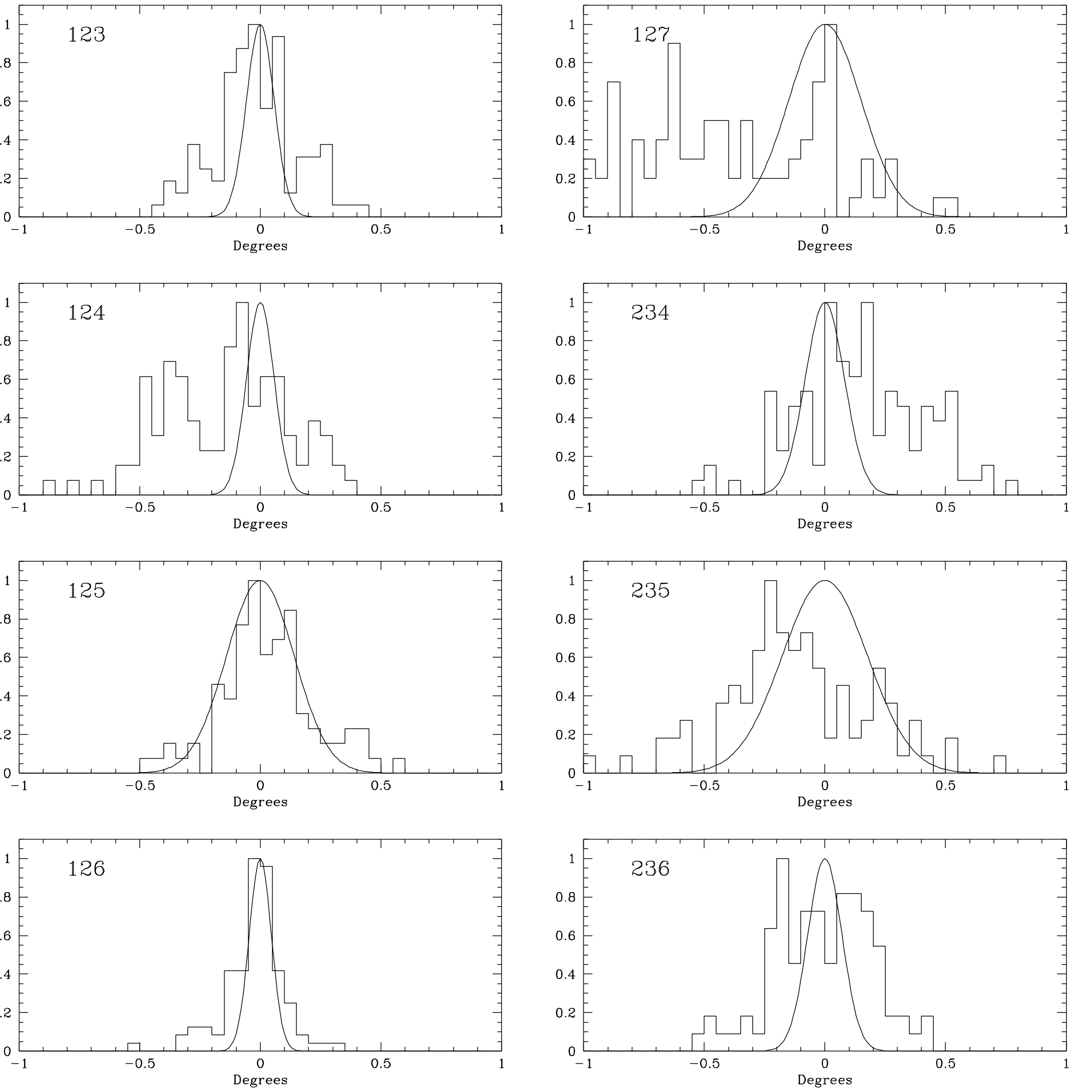

Fig. 3.— Histograms of the observed closure phases and predicted Gaussian probability distributions (1=B, 2=J, 3=L,4=N,5=S,6=W,7=C)

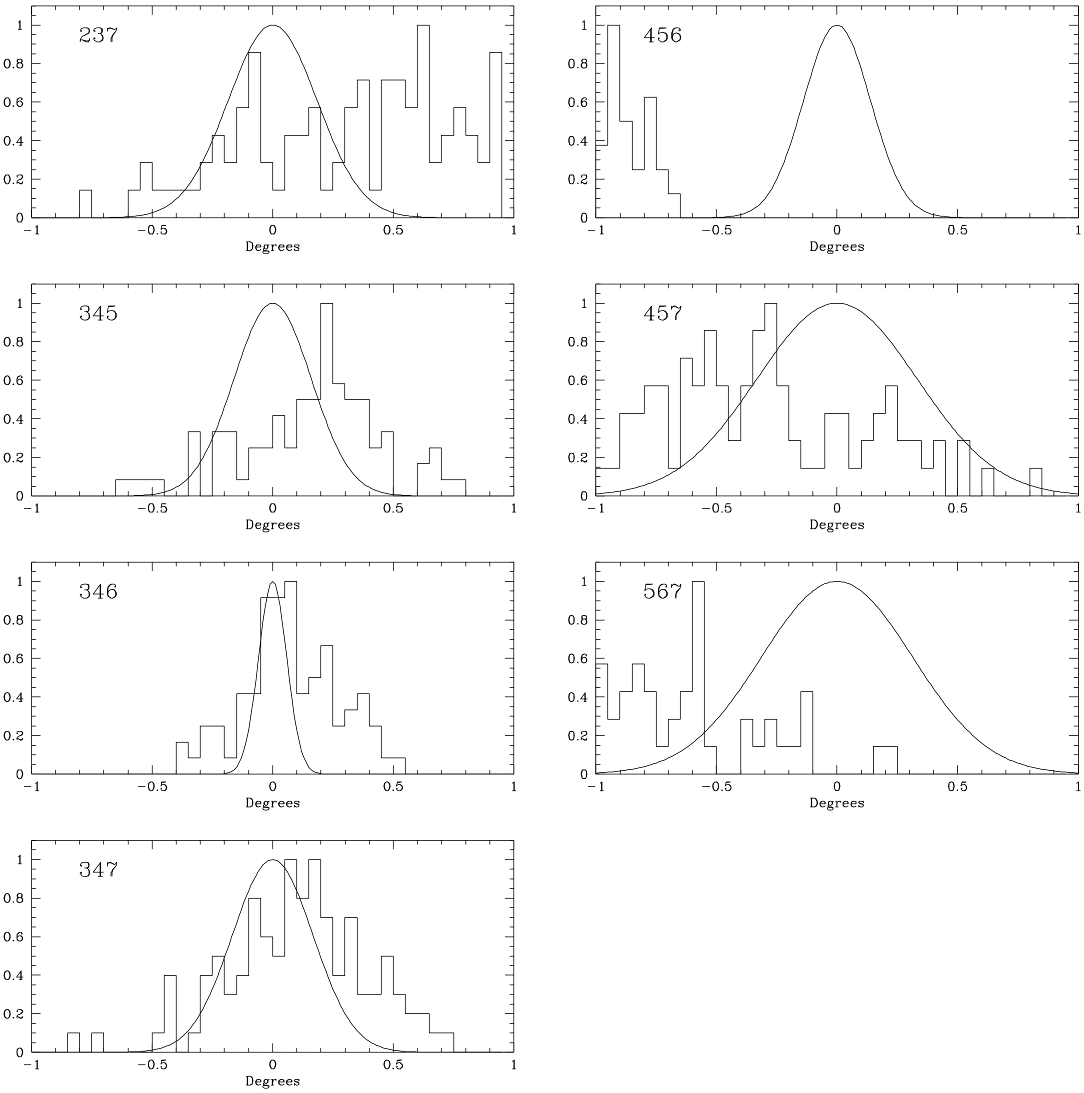
237
456
345
457
346
567
347
Degrees